



City Research Online

City, University of London Institutional Repository

Citation: Viridi, A. S., Zhang, Q., He, L., Li, H. D. & Hunsleys, R. (2015). Aerothermal Performance of Shroudless Turbine Blade Tips with Relative Casing Movement Effects. *Journal of Propulsion and Power*, 31(2), pp. 527-536. doi: 10.2514/1.b35331

This is the accepted version of the paper.

This version of the publication may differ from the final published version.

Permanent repository link: <https://openaccess.city.ac.uk/id/eprint/6024/>

Link to published version: <https://doi.org/10.2514/1.b35331>

Copyright: City Research Online aims to make research outputs of City, University of London available to a wider audience. Copyright and Moral Rights remain with the author(s) and/or copyright holders. URLs from City Research Online may be freely distributed and linked to.

Reuse: Copies of full items can be used for personal research or study, educational, or not-for-profit purposes without prior permission or charge. Provided that the authors, title and full bibliographic details are credited, a hyperlink and/or URL is given for the original metadata page and the content is not changed in any way.

City Research Online:

<http://openaccess.city.ac.uk/>

publications@city.ac.uk

AEROTHERMAL PERFORMANCE OF SHROUDLESS TURBINE BLADE TIPS WITH RELATIVE CASING MOVEMENT EFFECTS

A. S. Viridi and Q. Zhang*

Department of Engineering Science, University of Oxford, Oxford, UK, OX1 3JP
(* Currently University of Michigan-Shanghai Jiao tong University Joint Institute, Shanghai, China)

L. He

Department of Engineering Science, University of Oxford, Oxford, UK, OX1 3JP

and

H. D. Li and R. Hunsley

Rolls-Royce PLC, Bristol, UK, BS34 7QE

Qualitatively different heat transfer characteristics between a transonic blade tip and a subsonic one have recently been discovered. High resolution experimental data can be acquired for blade tip heat transfer research using a high speed linear cascade. A combined experimental and CFD study on several high pressure turbine blade tip configurations is conducted to understand the flow physics in both a stationary and moving casing setup. Extensive tests measuring aerodynamic loss and heat transfer have been performed on a stationary squealer tip at engine representative aerodynamic conditions. A systematic validation of the CFD solver (Rolls-Royce HYDRA) is introduced, showing good agreement with the experimental data obtained. Relative casing movement effects are then evaluated for two tip configurations at three different tip gaps. The moving casing is shown to affect the aerothermal performance considerably; the trends are consistently captured for the large and medium tip gaps, both in the stationary and moving casing instances. Presented results confirm that even with a moving casing, the blade tips remain transonic. It is also shown that the heat transfer is dependent on the tip gap size, but also the tip geometry configuration. The squealer cavity is subsonic regardless of the tip gap size, whilst the local flow state over a flat tip is much more responsive to tip gap size.

Nomenclature

C_{p0}	=	Total Pressure Loss Coefficient
C_x	=	Axial Chord (m)
g	=	Tip Clearance (m)
γ	=	Specific Heat Ratio
h	=	Heat Transfer Coefficient (W/m^2K)
M	=	Mach number
P	=	Pressure (Pa) or Pitch (m)
\dot{q}	=	Heat Flux (W/m^2)
R	=	Span-wise Direction (m)
ρ	=	Density (kg/m^3)
S	=	Blade Span (m)
T	=	Temperature (K)
v	=	Velocity (m/s)
x	=	Axial Direction (m)
y^+	=	Non-dimensional Wall Distance
y	=	Circumferential Direction (m)

(Subscripts)

0	=	Stagnation/total
ad	=	Adiabatic
e	=	Exit
i	=	Inlet
s	=	Static
w	=	Wall/Surface

I. Introduction

SHROUDLESS high pressure (HP) turbine blade tips are subjected to undesirable over-tip leakage (OTL) flow within the gap between the rotor blade tip and casing endwall, and are prone to high heat loads.

Several approaches have been taken to minimize the effects of OTL, for example, tip clearance control and seal segmenting. Tip design has been studied by many research groups and various tip configurations have been considered, such as flat, squealer and winglet tips. However, shroudless blade tips continue to be a challenge due to the level of complexity involved in understanding and prediction of the relevant flow physics, and their impact on aerothermal performance.

The basic understanding of tip aerothermal behavior has been so far largely based on two kinds of experimental setups: a) stationary cascade, and b) rotating rigs. Further classifications can be made in terms of the operation flow conditions: a) low speed and b) high speed. The simplest setup is a low speed cascade where detailed and accurate data can be relatively easily obtained. On the other hand, the most realistic environment is provided by a full rotating rig at a transonic condition, costly to build and difficult to instrument. The suitability of using a low fidelity setup can only be justified if the data/information gathered can serve the purpose of enhancing understanding and predictability of the flow physics relevant to the performance of interest. In this context, the following review should be able to firstly illustrate the extent of the influence that low speed cascades have had on the conventional wisdom in tip heat transfer. Secondly, attention is drawn to how this low speed flow based wisdom has been challenged by some recent work in high speed tip heat transfer. The realization of the importance of high speed conditioning naturally underlines the need of these high speed full rotating set ups. It also raises the stake of a more specific question in relation to the value of a transonic high speed cascade, leading to the motivation of the present work.

Early findings on high pressure turbine blades were presented in a comprehensive review by Bunker [1], summarizing and outlining the complex aspects with shroudless turbine design. Bunker et al. [2] presented detailed tip heat transfer measurements. They observed that reduced tip clearances can reduce heat transfer and located areas of high heat transfer. The work was complimented by a numerical analysis by Ameri and Bunker [3].

Practical studies on the squealer design were conducted by Bunker and Bailey [4]. They showed that deeper cavities can reduce tip heat transfer. Azad et al. [5, 6] also showed the improvements of a attaching a squealer compared to a flat tip. Furthermore, they discussed different squealer arrangements and outlined their effects on tip heat transfer. A single, rather than a double squealer, was shown to have lower overall heat transfer. Additional work on squealer tips includes those by Kwak et al. [7], Newton et al. [8], and Nasir et al. [9].

An analysis and interpretation of rotor blade heat transfer was given by Ameri and Steinhorrson [10]. Their predictions presented high heat transfer near the pressure and suction side edges and explained it by flow entrance effects. Ameri et al. [11] numerically studied plain and recessed tips. The inclusion of a casing recess showed positive signs of reduced tip heat transfer, however, a small effect on the aerodynamic efficiency. Additional validated numerical studies by Krishnababu et al. [12] and Yang et al. [13, 14] showed noticeable reductions of the tip leakage vortex and tip heat transfer with the squealer tip.

However, a major factor missed in a stationary cascade setup for aerothermal tip research is the effect of relative casing movement. Low-speed experimental studies using a moving belt were conducted by Yaras and Sjolander [15] showing a substantial reduction of tip gap flow. Tallman and Lakshminarayana [16] used simulations showing the implications of reduced gap flow and its effect on the tip leakage vortex. They noticed reduced tip leakage vortices, but also enhanced secondary flows. Krishnababu et al. [17] studied flat and squealer tips, showing that moving casing lowered averaged tip heat transfer on the squealer tips, but their flat tip only responded likewise at a smaller tip gap. The squealer geometry detailed aerothermal improvements over the flat tip. Similar effects were also recognized by Yang et al. [18]. Rotating effects acted to reduce averaged heat transfer and the squealer proved more beneficial. Furthermore, Mischo et al. [19] studied a modified squealer under moving casing and noticed aerothermal improvements over a flat tip. Moving casing effects on a modern winglet were sought by Zhou et al. [20]. They showed moving casing reduced tip gap flow thus reducing the tip heat transfer. The addition of a scraping vortex was also shown to alter the flow field downstream.

All of the above reviewed research is of a low speed nature and the majority of the tests and computational validation exercises are conducted in low-speed linear cascades. The data is valuable in helping to understand the physical flow features, their heat transfer impacts and in validating computational models. In fact these low speed data, analyses and the observations gather have formed the basis for the conventional wisdom.

High-speed research at engine realistic conditions tends to be difficult and capturing detailed tip heat transfer measurements is an on-going challenge. Dunn and Haldeman [21] measured tip heat fluxes at engine realistic conditions in a transonic rotating rig using film gauges. Thorpe et al. [22] measured heat transfer rates along a camberline of a transonic rotor blade and although in-line with early linear cascade tests, noticeable differences to low-speed work were spotted. Molter et al. [23] and Tallman et al. [24] combined numerical and experimental studies on tip heat transfer, providing some valuable data and predictions. It is recognized that these high speed full

rotating rig tests provide the highest experimental fidelity in a research environment and they will continue to provide important basis for validations of new design and computational methods developments. For tip research though, there remains to be challenging in providing easily accessible data from a high speed rotating rig at least on two counts: a) the challenge in getting detailed spatially resolved instrumentation and data, and b) providing an easily definable and adjustable inflow condition for a rotor row so that different factors (e.g. inflow turbulence, temperature) for the blade tip can be examined in isolation before putting everything together in a complex unsteady inflow environment in a full transonic stage. It might be argued that the value of these high speed transonic rigs may not be truly appreciated unless the necessity of a transonic flow condition is appreciated. The dominance of those low speed flow data in influencing the conventional wisdom indicates that the role of a transonic flow played in blade tip heat transfer had not been quite appreciated.

The appreciation of the transonic flow effect on blade tip heat transfer has been significantly enhanced by some recent findings, revealing distinctive aerothermal behavior in a transonic tip. Wheeler et al. [25] showed tip flow to be largely transonic and significantly different to low-speed cascade tests; showing almost the opposite in spatial trends. Experimentally, Zhang et al. [26] illustrated that the local heat transfer was directly affected by shock waves in a striped pattern within the tip gap. Zhang and He [27] also explored the differences of low and high-speed flows noting the difference in flow structures and tip leakage loss. Comparable findings were presented by Shyam et al. [28]. Further high-speed work led to similar findings on a flat tip by Zhang et al. [29], and a winglet tip by O'Dowd et al. [30]. Zhang and He [31] further illustrated a tip-shaping technique that would locally accelerate flow to reduce the local heat transfer, based on a concept instigated by He et al [32]. Additional tip-shaping trials were conducted by Shyam and Ameri [33] by trying to manipulate the shock-boundary layer interaction.

The recent observations regarding the distinctive high speed tip aerothermal characteristics, where a significant part of which were based on linear cascade testing, have underlined the need to address the moving casing issue at a high speed condition. A common limit to the previous moving casing studies is that they were mainly at low speed conditions. Although there are some preliminary indications of the relative moving casing effects in some recent publications of the authors' group [29], [30], there is a clear lack of analyses for systematic identification and understanding of the impact of relative casing movement and underlined mechanisms.

The present paper aims to address the lack of detailed aerothermal measurements on a squealer tip in a high speed linear cascade as well as the moving casing issue at a high speed condition. To the authors' knowledge, it is

the first time a squealer tip has been validated using the HYDRA solver under transonic flow conditions. Given the extensive previous comparative studies in various tip configurations, an emphasis is placed on examining moving casing effects and its sensitivity to tip geometry configurations. Specifically, a squealer and flat tip are considered in the present work.

The approach taken is to first carry out experimental measurements and conduct a systematic validation of the CFD solver adopted, before a computational study of the moving casing effect.

The rest of the paper is organized so that the experimental facility, instrumentation and the computational method is first introduced in Section 2. The validation study is presented in Section 3. The moving casing effects are examined for the squealer and a flat tip in Sections 4 and 5 respectively. The overall performances are analyzed and compared in Section 6 before the conclusion of the paper.

II. Methodology

A. Experimental Apparatus and Setup

Experiments are conducted in the Oxford University High-Speed Linear Cascade (HSLC) testing facility, a blow-down type wind tunnel. The test section consists of 5 blades and 4 passages with adjustable tip gaps and boundary layer bleeds. A moveable tailboard is attached to the sidewall to improve the periodicity. Table 1 lists the flow conditions measured for the present study.

Table 1 HSLC flow conditions for present study

Inlet Mach number	0.3
Inlet Reynolds number (based on Cx)	0.6×10^6
Exit Mach number	1
Exit Reynolds number (based on Cx)	1.3×10^6

Heat transfer measurements are taken on the tip surface of the centrally located blade. A transient measurement technique is used to determine local heat transfer coefficients (O'Dowd et al. [34]). A heater mesh located upstream of the test section provides a step-wise increase in mainstream flow temperatures of approximately 25°C.

Blade tip surfaces are made from an epoxy resin using a stereolithography technique for its low thermal conductivity property. A 25 μm diameter, fast response thermocouple is located on the tip for an in-situ calibration of infrared images. Heat transfer is modelled using a semi-infinite, solid conduction analysis. A Zinc Selenide (ZnSe) window is placed within the casing wall and provides optical access to the tip. A FLIR A20M infrared camera is used to record spatially resolved surface temperature measurements into a digital file simultaneously with

tip surface temperature readings. Equipped with a FireWire 400 data cable, the camera supplies an 8-bit greyscale output at a resolution of 160 x 120 at 30 frames per second. A linear temperature range of 0-50°C is used.

The temperature-time traces allow for a complete heat flux reconstruction at each pixel location and this is done using an Impulse method developed by Oldfield [35]. This reconstruction is described by O'Dowd et al. [34]. The linear relationship between tip heat flux and wall temperature during each blow-down run determines local heat transfer coefficients (1).

$$\dot{q} = h(T_{ad} - T_w) \quad (1)$$

Aerodynamic measurements are taken at 1 axial chord downstream of the blade row, parallel to the blade metal exit angle. A two-dimensional traverse system is employed to take total pressure measurements at uniform pitch-wise and span-wise locations. All measurements are taken from the same initial pitch-wise position at each radial position. Measurements at the exit plane are taken at 27 equally spaced pitch-wise and 6 span-wise locations, covering 77% to 96% of the engine equivalent blade span and one blade pitch. A three-hole probe is used to take these measurements up to 4 mm from the endwall due to the size of the probe.

Inlet measurements are taken using a pitot-static tube and thermocouple. Static pressures on the hub and casing are also measured at the exit. An inlet turbulence grid is installed upstream of the blade row. Measurements using a hot-wire probe show that the turbulence intensity ranges from 7-9%. Further details are provided by Zhang et al [37]. The same turbulence grid has been installed for the present study. Instrumentation used in the present study is shown in Figure 1.

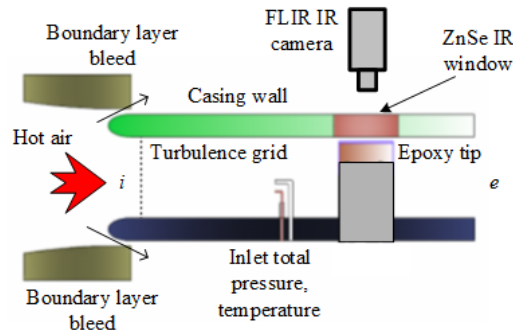


Figure 1 HSLC Instrumentaion

B. Experimental Uncertainties

Measurement uncertainties for the heat transfer taken using the Impulse method are discussed by O'Dowd et al. [34]. Since the apparatus and setup are essentially identical, the quantified uncertainties are also valid in the present

study. The overall uncertainty for the heat transfer coefficient is estimated to be within the range of $\pm 9.5\%$ and $\pm 1.2\%$ for the adiabatic wall temperature. The estimate takes into consideration of the material properties and measurements of the mainstream gas and wall temperatures.

The uncertainty associated with the aerodynamic loss has been conducted by O'Dowd et al. [36]. Again, since the testing facility and apparatus used are identical, the estimated uncertainty is also valid here. They estimate the uncertainty in the total pressure at $\pm 2.8\%$.

The uncertainty for the turbulence has been estimated by Zhang et al. [37] and they give an uncertainty of the turbulence intensity as approximately $\pm 0.5\%$ and about 1mm for the length scale.

C. Computational Method and Setup

Numerical predications are carried out using the Rolls-Royce HYDRA suite. The core of the software is a preconditioned, time marching, Reynolds-averaged Navier-Stokes equations (RANS) solver. The equations are discretized in space using a 2nd order, edge based finite volume scheme and integrated in time using a multi-stage Runge-Kutta scheme. Steady RANS calculations are performed and the Spalart-Allmaras (SA) turbulence model is adopted as the SA model provides the closest agreement with the experimental data. Similar results were discussed by [25]. The computational domain is based on one blade passage with periodic boundary conditions. The squealer blade definition and tip clearances are kept exactly the same as the experimental setup. Flow angle, turbulence intensity, stagnation pressure and temperature are matched at the inlet and the exit static pressure is matched at the outlet.

Mesh generation is done using Pointwise software. The mesh is of a multi-block, structured type with 7.7 million mesh cells with 50 grid lines within the tip gap. An additional 4.2 million cells are required to create the squealer tip in comparison to the flat tip mesh used in this study. Blade surface y^+ values are largely between 1 and 3. Isothermal wall boundary conditions are applied to wall surfaces with an exception to the hub, where an inviscid boundary condition is applied. Heat transfer coefficient (HTC) distributions are obtained using two solutions with two different wall temperatures and solving (1) for the HTC using simultaneous equations. Grid independence is established as a further increase in mesh density shows negligible change to surface heat flux values. Visualizations of the HYDRA solutions are done using Matlab, Paraview and Ensign.

III. Validation study (Experiment vs. CFD)

Squealer tip heat transfer and exit total pressure measurements obtained from the experiments are presented in this section for three different tip gaps (0.5%, 1% and 1.5% of the blade span). The tip gap is defined from the casing wall to the top of the squealer rim. HYDRA predictions follow and are used as part of the validation exercise.

A. Tip Heat Transfer

Tip heat transfer results are presented in Figure 2 (a). Results shown are experimental, spatial distributions of HTC on the squealer tip for three tip gaps ($g/S=0.5\%$, 1% and 1.5%). The frontal cavity region shows an increase of HTC as the tip gap is increased; in-line with previous high-speed research. The squealer suction side rim show high levels of heat transfer that increase with larger tip gaps.

HTC contours from HYDRA predictions are shown in Figure 2 (b). Results are in close agreement with those experimentally determined. The main heat transfer patterns are clearly detected, within the cavity and on suction side rim. CFD predictions capture the features well, both locally and overall.

Figures 3 (a) and (b) show circumferentially-averaged HTCs for the three tip gaps presented. There is a general reduction of averaged heat transfer as the tip gap reduces in size. Notice also, at smaller tip clearances (experimentally and numerically), a higher averaged heat transfer is observed towards the trailing edge. Overall averaged tip HTCs, measured and predicted, are provided in Table 2.

Table 2 Mean tip heat transfer coefficients

Tip Gap (g/S)	HSLC HTC [W/m^2K]	HYDRA HTC [W/m^2K]
0.5%	1012.6	1025.4
1%	1122.0	1107.2
1.5%	1228.0	1136.6

The trends shown suggest that local heat transfer is largely affected by tip clearance size when the local flow is subsonic. In this region (0-60% C_x) HTC decreases with a reduction in tip gap. Where it is transonic, changes are less obvious. For the near trailing edge region, an opposite trend is observed. As such, there is a cross-over point in the HTC-tip gap variations around 80% C_x . This is more apparent with the HYDRA data. The change of the gap dependence behavior is well captured by both the experiment and CFD. Similar cross-over behavior was reported for a flat tip by Zhang et al. [29].

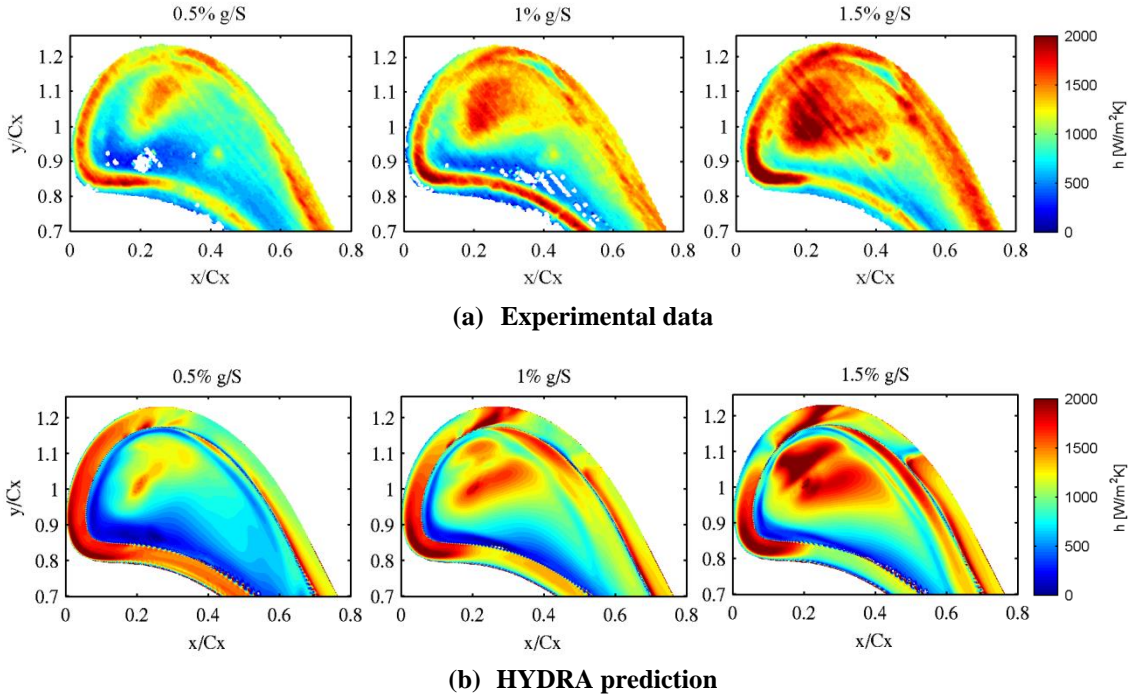


Figure 2 Squealer tip HTC contours for tip gaps 0.5%, 1% and 1.5% g/S (HSLC & HYDRA)

HYDRA predictions detect the local variations in heat transfer on the squealer tip. The trends associated with the tip gap variations are very consistent and compare well with the experimental data, falling within the quoted uncertainty bounds of $\pm 9.5\%$. In Figure 3, this is largely the case; however, noticeable differences are identified. The leading edge heat transfer follows a different trend and HYDRA shows the peak HTC at the leading edge (0-10% C_x). This discrepancy lies mostly with the smallest tip gap, where experimentally, accurately positioning the blades and measuring a tight tip clearance of 0.5% g/S has a significant source of error associated with it. Larger discrepancies are seen towards the trailing edge of the blade where three-dimensional conduction effects dominate.

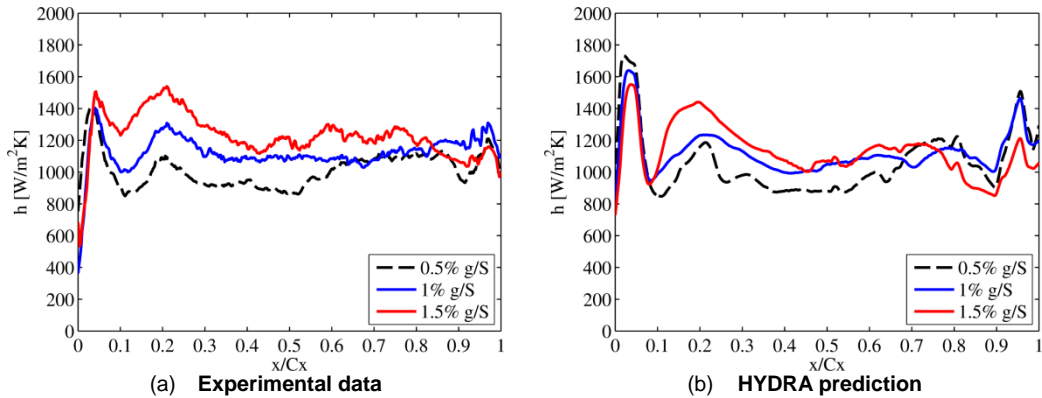


Figure 3 Squealer tip circumferentially-averaged HTC along axial chord for experimental and numerical results (HSLC & HYDRA)

B. Aerodynamic Loss

In the present study, the total pressure loss coefficient is used to determine the aerodynamic loss performance. Experimentally, total pressures are obtained by using the three-hole probe at the exit plane, one axial chord downstream of the trailing edge. This is also numerically calculated by HYDRA, at the same exit plane, and directly compared to those measured. The total pressure loss coefficient Cp_0 is defined by equation (2).

$$Cp_0 = \frac{P_{oi} - P_{oe}}{0.5\rho v^2} = \frac{P_{oi} - P_{oe}}{0.5\gamma P_s M^2} \quad (2)$$

The denominator represents the exit dynamic pressure. This value is determined by mass-averaging local dynamic pressure along the mid-span of the cascade at the exit, one axial chord downstream of the blade row. Static pressures are determined using the isentropic relationship between obtained Mach numbers and total pressures.

Experimentally obtained total pressure loss coefficient Cp_0 distributions are shown in Figure 4 (a) for all three tip gaps.

The results presented in Figure 4 (a) illustrate typical tip leakage flow features. In general, as the tip gap increases, there is an increase in tip leakage flow and therefore, a larger OTL vortex. The results show this trend occurring at the defined exit plane. Higher loss is created with the growth of these vortices. Another aerodynamic development is the shifting of this vortex as the gap increases. The contour plots show that as the tip gap becomes larger, the vortex shifts away from the blade suction surfaces.

Numerically predicted total pressure loss coefficient distributions for the three tips gaps determined by HYDRA are shown in Figure 4 (b). The comparison with the experimental results shows good agreement, both in terms of the OTL vortex size as well as the pitchwise shifting of these vortices.

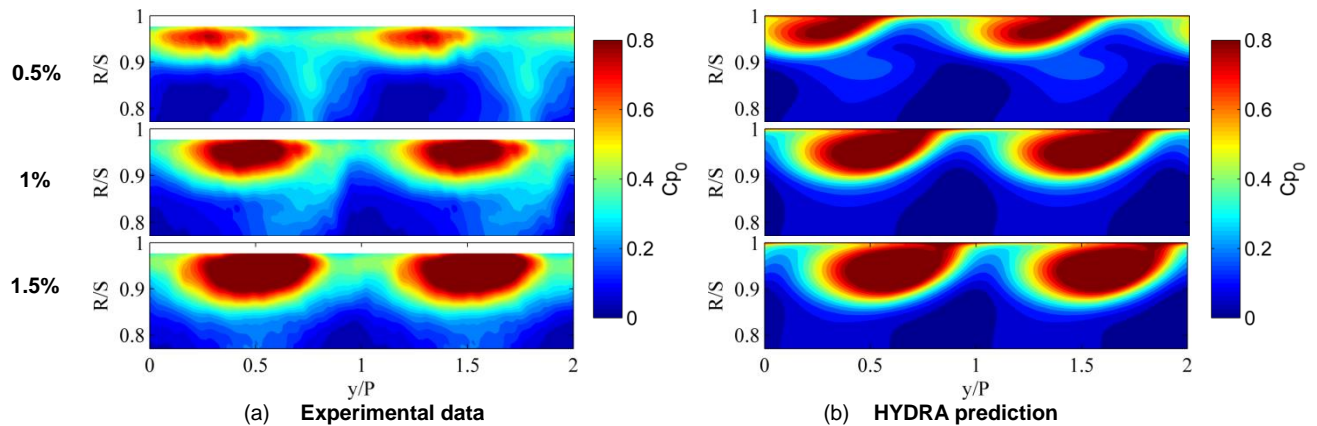


Figure 4 Squealer tip total pressure loss coefficients Cp_0 for tip gaps: 0.5%, 1% and 1.5% g/S (HSLC & HYDRA)

Pitchwise-averaged C_{p0} plots are presented in Figure 5 for the three tip gaps and Figure 6 shows overall mass-averaged total pressure losses. Overall, in terms of validation exercise, the experimental and numerical predictions agree quite well. The mean heat transfer coefficients give percentage errors between the measured and predicted results of 1.2%, 1.3% and 8.0% for the 0.5%, 1% and 1.5% tip gaps respectively. These fall within the estimated experimental uncertainty range. The overall aerodynamic loss percentage errors are 13.6%, 4.8%, 2.0% for the 0.5%, 1% and 1.5% tip gaps respectively. The largest discrepancy is observed with the tightest tip clearance and difficulty in measuring the gap accurately. Also, the measured losses for the two smaller gaps indicate the formation of a passage vortex ($0.5 < y/P < 1$) seen in Figure 4 (a), which is not well detected numerically.

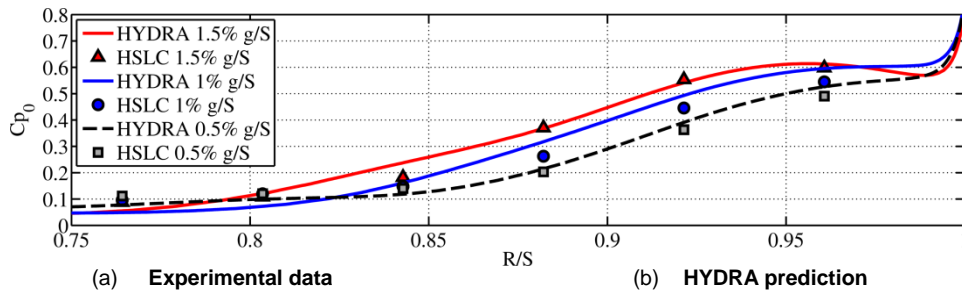


Figure 5 Squealer tip pitchwise-averaged total pressure loss C_{p0} for tip gaps: 0.5%, 1% and 1.5% g/S (HSLC & HYDRA)

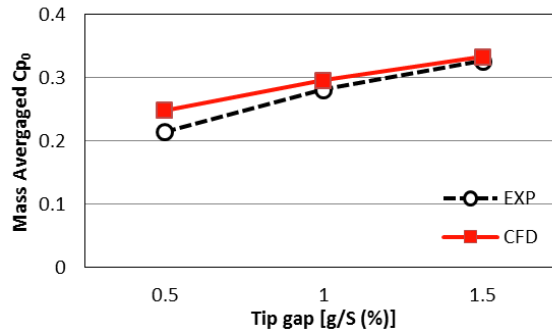


Figure 6 Mass-averaged total pressure loss variations with tip gap 0.5%, 1% and 1.5% g/S (HSLC & HYDRA)

IV. Squealer Tip with Moving Casing

Having validated the CFD solver’s capability for heat transfer and aerodynamics loss predictions for a stationary cascade condition, we now examine the moving casing effect. In the HYDRA calculations, the relative casing motion is simulated by specifying a tangential velocity of the casing wall boundary in a direction from the suction side to pressure side of the blade.

A. Tip Heat Transfer

Figure 7 shows heat transfer coefficient maps for the three tip gaps considered under a moving casing. The basic patterns shown in Figure 7 are noticed to be comparable to that with a stationary wall (Figure 2 (b)). In particular, the cavity region nearest the leading edge, where flow is impinging. Furthermore, the pressure side rim shows relatively little variation when compared to the case with a stationary casing wall.

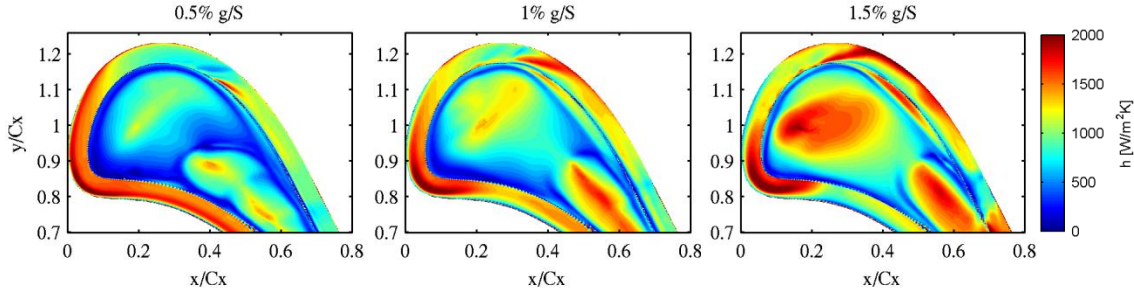


Figure 7 Squealer tip HTC contours for tip gaps (0.5%, 1% and 1.5% g/S) with moving casing employed (HYDRA)

However, some noteworthy changes are identified. A region of high heat transfer is formed within the cavity at approximately 40%-70% C_x . This area follows a pattern similar to the leading edge, subsonic, cavity region, whereby a decrease in tip gap reduces the heat transfer. This is qualitatively in line with the commonly held view based on the low speed tests that a reduction of leakage flow at a smaller gap leads to a lower heat transfer.

To illustrate this phenomenon more clearly, streamlines are drawn for both the stationary and moving endwall scenarios for 1% tip gap shown in Figures 8 (a) and (b). The streamlines give an insight into the newly formed hot spot within the mid-cavity region. The moving casing wall pulls fluid in the tangential direction. The orientation of the cavity slot at the mid-chord position is such that the friction pulling force seems to help the formation of the in-cavity vortex in two ways: firstly, by promoting a reattachment inside the cavity and secondly, by enhancing the vortex core fluid movement along the cavity, which in turn strengthens the vortex itself. As a result, the over-tip fluid in this region is wrapped into a strong and compact vortex inside the cavity rather than continually flowing over the cavity and the suction side rim as in the stationary cascade case. The hot spot region in the mid-cavity between 40-70% C_x (Figure 7) is thus identified to be caused by the heat transfer augmentation due to the impinging flow of the mid-cavity vortex.

It should be emphasized that a similar vortex impingement with the corresponding heat transfer impact occurs in the frontal main cavity area. The comparison in tip heat transfer between the stationary casing (Figure 2) and the

moving casing (Figure 7) suggests that the moving casing seems to have a much smaller effect on this main frontal vortex impingement.

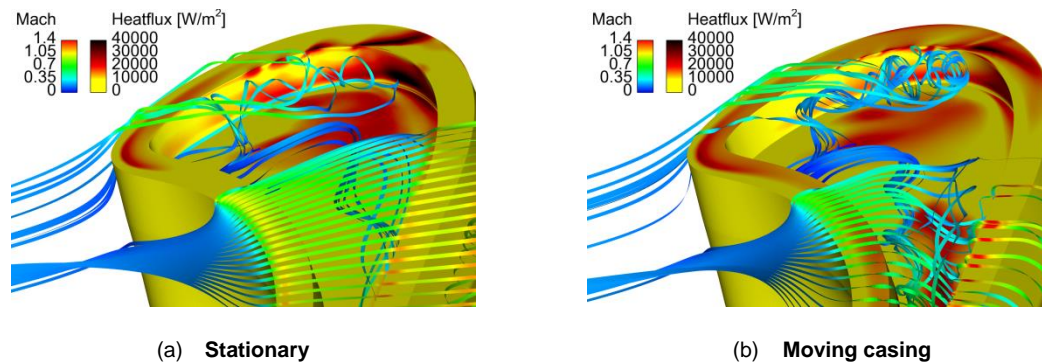


Figure 8 Streamlines showing over-tip leakage flow where blade and tip surface contours show heat flux and streamlines colored by Mach number for 1% tip gap cases (HYDRA)

Circumferentially-averaged HTC for the three moving endwall cases (Figure 9) broadly suggest that the local patterns of heat transfer are similar to those shown in the stationary case (Figure 3). As the tip gap is reduced, the reduction in HTC over the subsonic cavity region (10% to 40% C_x) is clear. The transonic part (70%-90% C_x) shows a wiggling behavior similar to its stationary counterpart (Figure 3b).

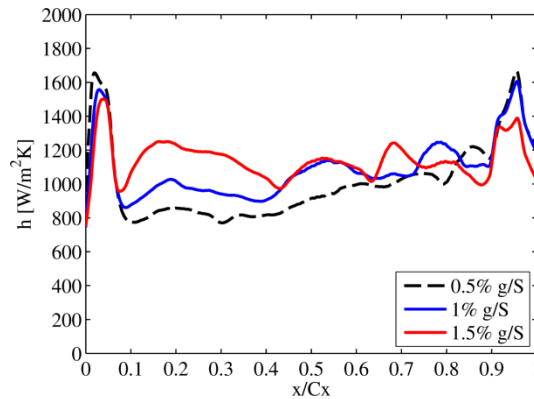


Figure 9 Squealer tip circumferentially-averaged HTC along axial chord with moving casing (HYDRA)

B. Aerodynamic Loss

Total pressure loss is now considered, as previously studied in section III, part B. Predictions of the loss are taken at the exit plane, one axial chord away from the blade trailing edge for the squealer tip. Contour maps of C_{p0} with moving casing for three tip gaps are shown in Figure 10.

Striking differences can be seen by comparing the pressure loss contours for the moving casing case (Figure 10) with those for the stationary casing (Figures 4, 5). The casing movement is seen to significantly promote the

passage vortex, which now has a much clearer loss core identifiable beneath that of the OTL loss core. Clearly the OTL vortex reduces in size and strength when the tip gap is reduced, as expected, while the passage vortex is much less sensitive to the tip gap size. The loss signatures of the passage vortex for the medium and large side are almost unchanged.

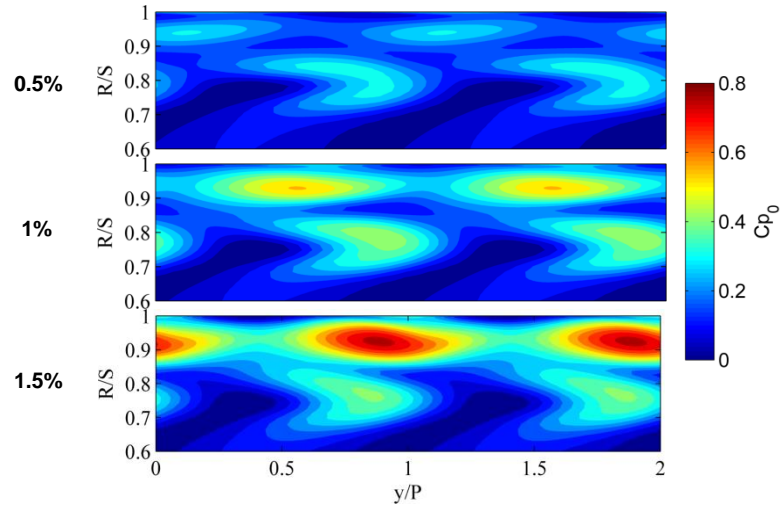


Figure 10 Numerical predictions of total pressure loss coefficient Cp_0 for squealer tip with moving casing for tip gaps 0.5%, 1% and 1.5% g/S (HYDRA)

Pitchwise-averaged Cp_0 comparisons for the 1% tip gap, stationary and moving casing cases are shown in Figure 11.

For the stationary cascade configuration, the loss core is dominantly influenced by the peak associated with the OTL vortex. On the other hand, for the case with the moving casing, there are two clearly identifiable peaks associated with the passage vortex and the OTL vortex respectively. Interestingly, the net contributions of the two interacting vortical flow structures for the moving casing are largely balanced out in comparison with that from the dominant OTL vortex for the stationary casing case. Further discussions on the net effects on the overall losses will be presented later in comparison with the performance for a flat tip.

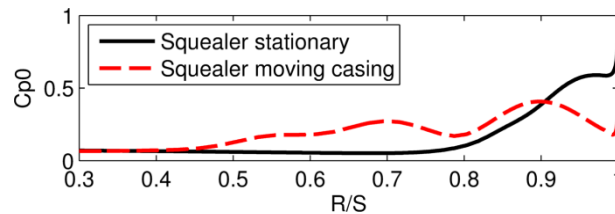


Figure 11 Pitchwise-averaged total pressure loss coefficients Cp_0 for the squealer tip with and without moving casing for the 1% tip gap (HYDRA)

V. Flat Tip with Moving Casing

In order to identify the sensitivity of tip gap design to relative casing motion, a flat tip is analyzed with a stationary and moving casing respectively. Aimed at a consistent comparison, the same blading profile and flow conditions are adopted as those of the squealer case. It is recognized that the loading near the tip will have to be tip-configuration dependent. For the present cases, the hub aerodynamic loading has been checked to be more or less the same for both tip configurations.

Heat transfer coefficient contour maps for the flat tip are presented in Figure 12, showing the stationary and moving casing results respectively.

Figure 12 (a) shows typical results for a flat tip at a transonic flow condition. A flat tip considered by Zhang et al. [29] showed a similar leading edge hot stripe that reduces with decreasing tip gap. In addition, the trailing edge becomes more thermally vulnerable at smaller tip gaps. These features are also clearly identified here. The subsonic behavior for the near leading edge region gives similar trends to the squealer tip where there is a reduction of heat transfer as tip gap reduces. On the other hand, as the tip gap reduces, there are higher heat loads towards the trailing edge. It becomes evident that the viscous force from the casing motion enhances this effect, suggesting a much larger subsonic region when adding the casing motion. To illustrate this further, local Mach number plots for the mid-gap region are presented (for the 3 tip gaps) in Figure 13. It confirms that the rear transonic region can be reduced in size by either a smaller tip gap or by the relatively moving casing.

Circumferentially-averaged heat transfer coefficient plots are shown in Figures 14 (a) and (b). It is clear that the heat transfer patterns are dependent on the flow regimes over the tip. The subsonic flow part shows a trend of decreasing heat transfer with smaller tip gaps (seen in the squealer case also). However, a cross-over region is seen, where these trends are reversed for the transonic part, noticed with both the stationary and moving casing cases. The basic cause for the opposite trends of the HTC-gap dependence for the subsonic and transonic regions is chiefly linked to the marked reduction of heat transfer in a transonic region, as pointed out by Wheeler et al. [25]. This is also the basis for the over-tip shaping to generate a high speed flow to reduce heat transfer by Zhang and He [31] and also reported by Shyam et al. [28] and Shyam and Ameri [33]. For a transonic region, the local flow will have to be reverted back to a subsonic state when the gap is small enough (top right of Figure 12), thus leading to an increase in heat transfer at a small gap.

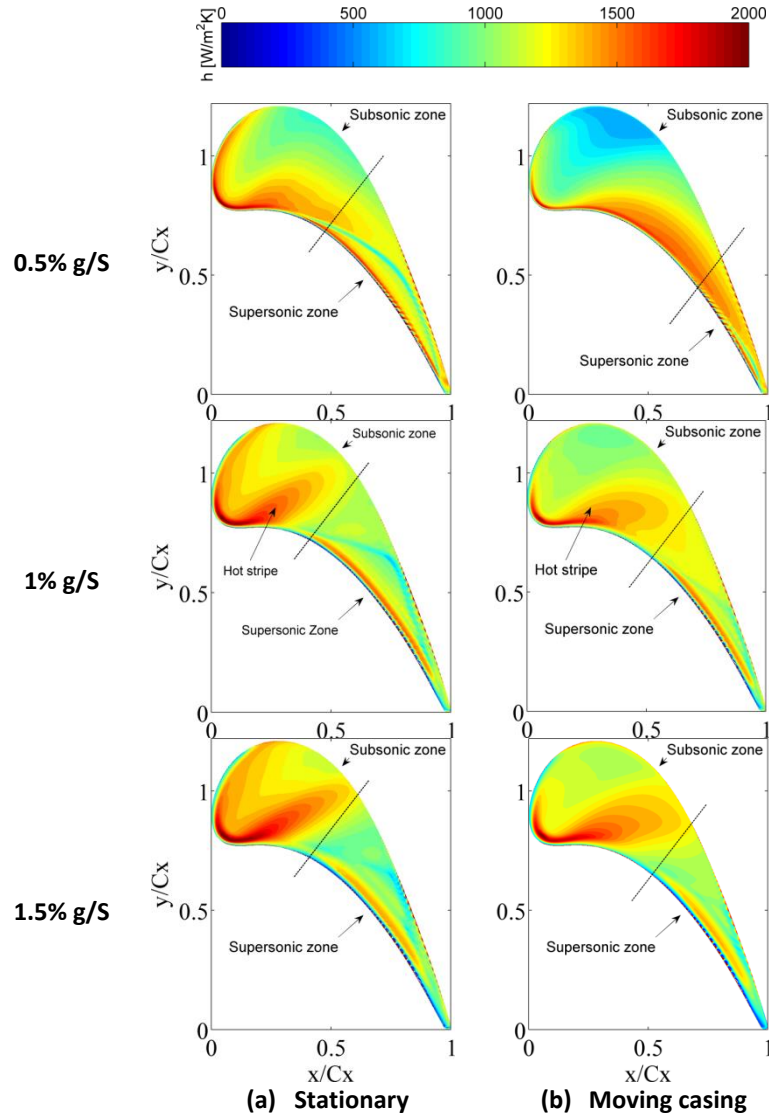


Figure 12 Flat tip HTC contours for tip gaps (0.5%, 1% and 1.5% g/S), stationary and moving casing (HYDRA)

The moving casing does not qualitatively change the overall opposite trends for the two flow regimes. Nevertheless, for all tip gaps considered, the transonic region over the tip is reduced in size when the moving casing is employed due to the extra casing friction (Figure 13), and hence a slightly more downstream position of the cross-over point from 55% Cx to 60% Cx , as indicated in Figure 14 (b).

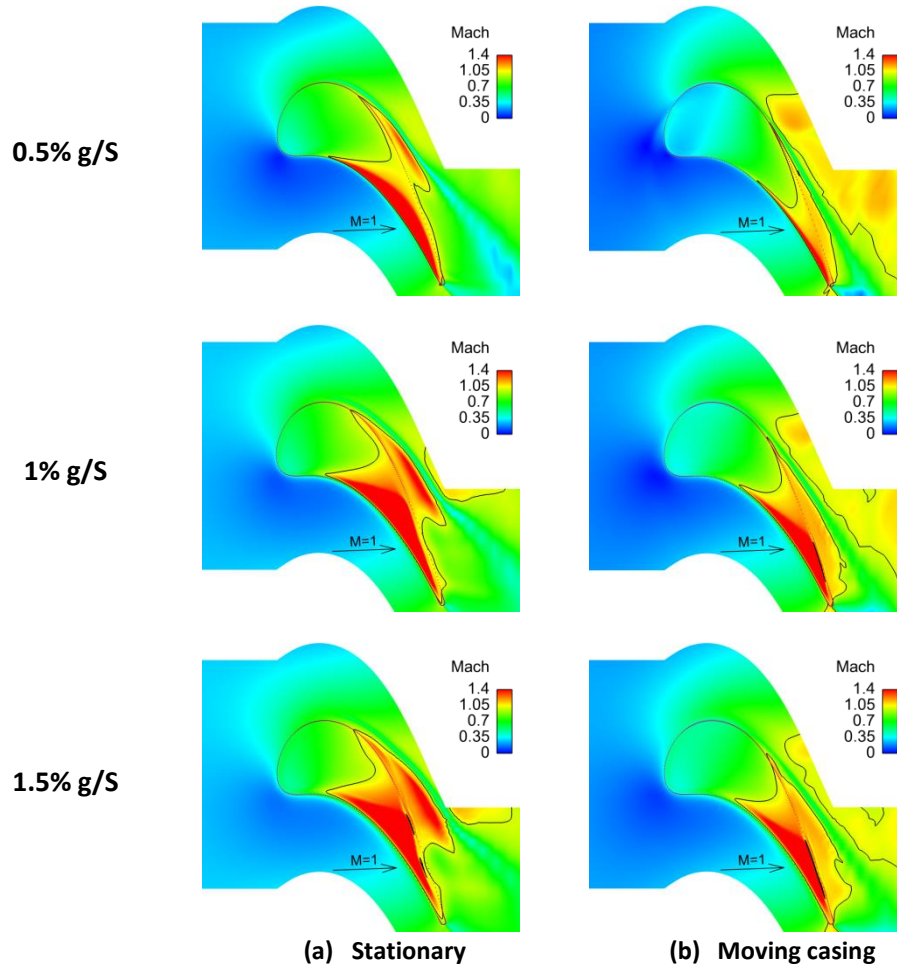


Figure 13 Local Mach number distributions on mid gap plane (solid line indicates Mach=1), flat tip (HYDRA)

Another interesting feature to note is that the heat transfer is seemingly non-proportionally changed at the small gap (0.5% span). In other words, there is a much larger difference between 0.5% gap and 1% gap than that between 1% and 1.5% gap. This non-proportionality was not observed for the squealer case, with either a moving casing (Figure 9) or a stationary casing (Figure 3). This difference in the HTC-gap dependence between the two geometry configurations is believed to be due to the fact that for a flat tip, the whole over tip flow is subject to a shear effect from casing with an equal distance, everywhere in the over tip region. On the other hand, for a squealer tip, the bulk of flow in the cavity is much farther from the casing, and hence less affected by its motion.

In addition to the tip heat transfer, the total pressure loss coefficients, C_{p0} , are also calculated and compared between the moving and stationary casing cases. The detailed results of the differences between the two casing boundary condition results (not shown here) are very similar to those for the squealer tip. Namely, with a moving casing, the over-tip leakage vortex is reduced in strength and the passage vortex is strengthened. Overall, it is seen

that a reduced tip gap does reduce the loss and the trend is consistent for all tip gaps, with and without the casing motion.

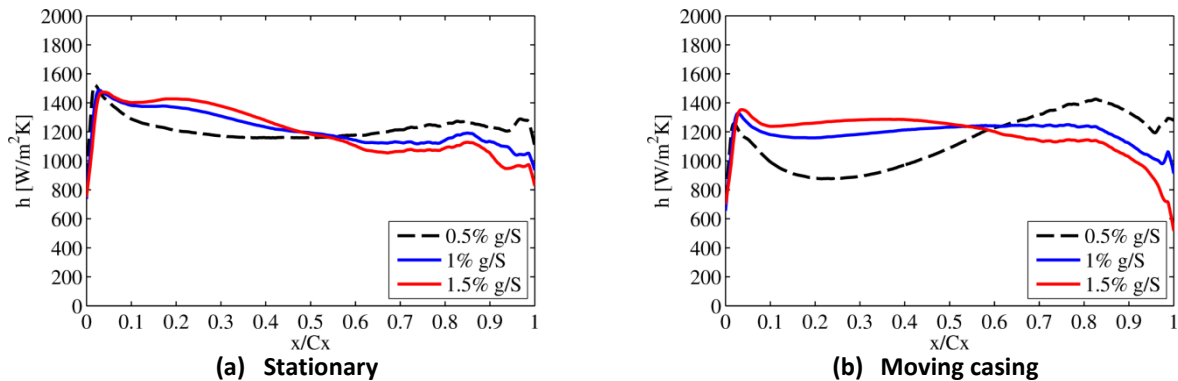


Figure 14 Calculated circumferentially-averaged HTC along axial chord for a flat tip (HYDRA)

VI. Overall Aerothermal Performance

Direct comparisons of the overall aerothermal performance between the two tip configurations are presented in this section. For heat transfer, overall tip surface averaged values of heat transfer coefficient are given. For aerodynamic losses, the mass averaged entropy rise at the exit plane is considered. The main question of interest is: can the results from a stationary cascade setup rank the performance differences (between different tip gaps and between different configurations) consistently?

A. Overall Heat Transfer Coefficient

The overall area-averaged tip heat transfer coefficient values for the squealer and flat tips are calculated and shown in Figure 15.

Firstly, it is noted that for the squealer tip, as the tip gap increases, the overall heat transfer increases. The trend is the same for both the moving and stationary casing cases. Although, for the large tip gap, the values with and without casing movement are almost the same, this is obviously a coincidence as the detailed spatial HTC distributions for the two cases are largely different (Figure 2, Figure 7).

On the other hand, the flat tip overall values for the stationary casing do not seem to suggest a clear trend. However, the results with the casing movement do show an increase in heat transfer with increasing tip gap. Following the discussion of the flat tip, the results at 0.5% gap are regarded as being dominantly influenced by the moving casing effect. Bearing this in mind, it can be seen that the results, at tip gaps of 1.0% and 1.5%, do follow the same trend for both the moving and stationary casing.

Comparing both tips, it is apparent that the squealer tip has lower overall HTC when compared to the flat tip, per tip gap. This observation also holds when the moving casing is applied. This suggests that with respect to heat transfer, the squealer is thermally advantageous over the flat tip, and based on previous research [30], the winglet.

It can be seen that the casing motion also lowers the overall HTC. Again this is consistently observed for all tip gaps.

Finally a cautionary note should be added here when comparing the overall average parameters. It is observed that the local changes for different configurations and casing conditions appear to be much more contrasting than those in terms of the averaged HTC. The averaged heat transfer parameter is adopted here simply as a compact and convenient indicator, which should not be over relied on without further examination as presented and discussed earlier.

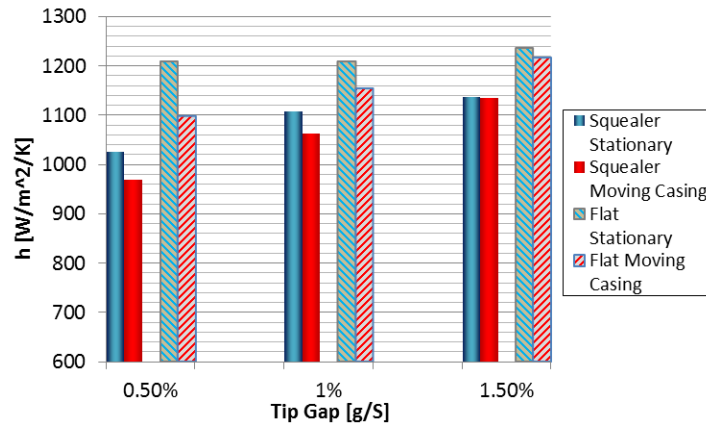


Figure 15 Area-averaged tip HTC for squealer and flat tips, with and without casing movement (HYDRA)

B. Overall Aerodynamic Loss/Entropy Rise

Since the moving casing applies work on the fluid, the overall entropy rise (instead of total pressure loss), taken at the exit plane of the computational domain, is used as a measure of flow losses to understand the performance of the two tip configurations at the 3 tip gaps. Results are presented in Figure 16.

The fundamental gap dependence behavior of the loss reduction with smaller tip gaps is clearly shown for both tip configurations consistently with or without the moving casing.

The comparisons between the two configurations are more complex. At the small tip gap (0.5%), the results with the moving casing still show a performance gain by the squealer over the flat tip, but those with a stationary casing do not. This abnormality is again attributable to the dominant influence of the casing movement at the small gap, which is much larger for the flat tip than for the squealer tip. Table 3 shows the percentage change of entropy rise

when a moving casing is applied. Focusing exclusively on the two larger tip gaps (1% and 1.5%), it is observed that adding moving casing provides an additional 17-18% rise in terms of the entropy function $[1-\exp(-dS/R)]$, consistent for both cases of the flat tip and squealer.

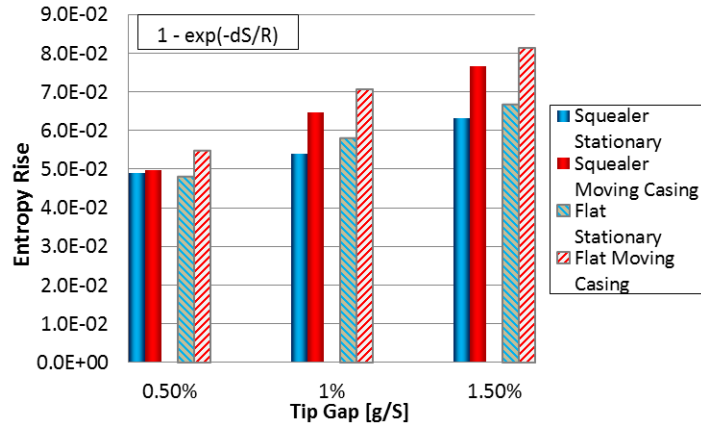


Figure 16 Overall entropy rise $[1-\exp(-dS/R)]$ for squealer and flat tips, with and without casing movement (HYDRA)

Furthermore, Table 4 shows the geometry effects and shows the percentage change of the entropy function when replacing a flat tip with a squealer tip, both with and without casing movement. For the two larger tip gap cases, the improvement of having a squealer tip is between 6-9% better than having a flat tip.

Table 3 Percentage change of entropy rise function when casing movement is applied to stationary case (Reference case is the moving casing)

Tip gap (g/S)	Squealer	Flat
0.5%	1.4%	11.9%
1%	16.5%	17.8%
1.5%	17.6%	18.1%

Table 4 Improvement of squealer over flat tip (percentage reduction of entropy rise function) (Reference case is the squealer tip)

Tip gap	Stationary	Moving Casing
0.5%	1.9%	-9.8%
1%	-7.5%	-9.2%
1.5%	-5.8%	-6.4%

C. Further Discussion

As stated in the introduction part, the main motivation of the present work is to identify, if and how, a stationary cascade configuration can be used for rotor blade tip design and analysis. The present results suggest that the moving casing effect depends on the geometry.

A flat tip seems to be more strongly dependent on the moving casing (Figure 14). A simple geometrical argument relates the influence on the over-tip flow to the uniformly short distance to the casing wall, when the gap is small. This should, to some extent, explain the non-proportionally large changes at the small tip gap, when the moving casing is introduced.

There is another distinctive tip-geometry dependent feature to be noted. In relation to the HTC-gap variation, there is a clear cross-over point in the mid-chord region (50%-60% C_x) for the flat tip, with or without the moving casing (Figure 14). For a squealer tip however, this cross-over point is located much more downstream (Figure 3, Figure 9). The cross-over point effectively separates the two regions with the opposite trends in HTC variation as the tip gap changes. Consequently, for a squealer tip, the overall trend of heat transfer variation with the tip gaps is clearer and less influenced by other factors including the strong shearing effect due the casing motion as seen with a flat tip. The reason for the contrasting behavior with different tip geometries can be attributed to the differences in flow regime of the bulk over-tip flows between the two tip configurations. For a flat tip, the rear part of the transonic flow at a large tip gap will have to revert back to a subsonic state at a very small tip gap. For a squealer tip however, the bulk of the over-tip fluid is trapped inside the cavity, and will remain to be subsonic regardless of what the flow state over the pressure side or suction side rims may be in. This bulk of subsonic flow within the main squealer cavity would dictate the overall gap dependence behavior of the squealer tip. It thus results in a more proportional change of HTC at a small tip gap as we have observed (Figure 3, Figure 9) than its flat tip counterpart.

A linear cascade is able to provide high resolution spatial tip heat transfer data and a detailed map of the aerodynamic loss. Linking this environment to a rotating one proves to be complex and basing results on a linear cascade is challenging. The sensitivity of the moving casing (results not presented here) is not as straightforward as expected, but knowing there is a dependence on the tip geometry and that tip flow under both scenarios remains transonic may help assist with future research and the design of turbine blade tips in a rotating setting.

VII. Conclusions

The present work starts with an experimental validation for a shroudless blade tip configuration in a linear cascade set up at engine realistic transonic aerodynamic conditions. Infrared thermography based heat transfer measurements and aerodynamic loss traverse data have been obtained. The HYDRA RANS solutions are shown and compare well with the experimental data. The hot spots and high local gradients over the tip surface as observed in both the experiment and CFD underline the need for spatially resolved heat transfer measurement and prediction.

Extensive CFD analyses are directed to examine the effects of relative casing motion. The results show that the relative casing movement affects the detailed near-tip aerothermal field considerably. Importantly, the present results demonstrate that a significant portion of the over-tip flow remains transonic, with or without the moving casing. The gap dependence of the over-tip heat transfer clearly shows opposite trends for the transonic and subsonic regions respectively.

Furthermore, the moving casing effects are shown to be markedly dependent on both the tip gap size and the tip geometry configurations. For three tip gaps (0.5%, 1.0%, 1.5% span) considered, the overall heat transfer and aero-losses for the medium and large gaps are consistently ranked for both the squealer and flat tip, with or without the moving casing. At the small tip gap, the over-tip flow for the flat tip is much more strongly affected by the moving casing due to the uniformly close proximity to the casing wall. In addition, there is a significant difference in the flow state, contributing to the different HTC-gap variations. The bulk fluid in the squealer cavity is always subsonic regardless of the tip gap size; hence the squealer tip exhibits a more proportional variation of heat transfer with tip gap size than a flat tip.

The overall observation is that a high speed linear cascade setup can certainly serve as useful validation vehicle. It is also shown to be able to consistently rank the overall tip aero-thermal performance for medium and large tip gaps. Caution will have to be exercised for a small tip gap, particularly restrictive for a flat tip.

VIII. Acknowledgement

The authors gratefully acknowledge the support of Rolls-Royce plc and EPSRC for funding this project.

IX. References

- 1 Bunker, R. S. A Review of Turbine Blade Tip Heat Transfer. *Annals New York Academy of Sciences*, 934 (2001), 64-79.
- 2 Bunker, R. S., Bailey, Jeremy C., and Ameri, A. A. Heat Transfer and Flow on the First-Stage Blade Tip of a Power Generation Gas Turbine: Part 1—Experimental Results. *ASME Journal of Turbomachinery*, 122(2) (2000), 263-271.
- 3 Ameri, A. A. and Bunker, R. S. Heat Transfer and Flow on the First-Stage Blade Tip of a Power Generation Gas Turbine: Part 2—Simulation Results. *ASME Journal of Turbomachinery*, 122 (2000), 272-277.
- 4 Bunker, R. S. and Bailey, Jeremy C. Effect of Squealer Cavity Depth and Oxidation on Turbine Blade Tip Heat Transfer. *ASME Paper No 2000-GT-0155* (2000).
- 5 Azad, G. S., Han, J. C., Boyle, R. J. Heat Transfer and Flow on the Squealer Tip of a Gas Turbine. *ASME Journal of Turbomachinery*, 122 (2000), 725-732.
- 6 Azad, Gm S, Han, J.C., Bunker, R. S, and Lee, C. P. Effect of Squealer Geometry Arrangement on a Gas Turbine Blade Tip Heat Transfer. *Journal of Heat Transfer*, 124(3) (2002), 452-459.
- 7 Kwak, J.S., Ahn, J.Y., Han, J.C., Lee, C.P., Bunker, R.S., Boyle, R.J., and Gaugler, R.E. Heat Transfer Coefficients on the Squealer-Tip and Near-Tip Regions of a Gas Turbine Blade with Single or Double Squealer.

- ASME Journal of Turbomachinery*, 125(4) (2003), 778-787.
- 8 Newton, P.J., Lock, G. D., Krishnababu, S. K., Hodson, H. P., Dawes, W. N., Hannis, J. and Whitney, C. Heat Transfer and Aerodynamics of Turbine Blade Tips in a Linear Cascade. *ASME Journal of Turbomachinery*, 128 (2006), 300-309.
 - 9 Nasir, H., Ekkad, S.V., Kontrovitz, D., Bunker, R.S., and Prakash, C. Effect of Tip Gap and Squealer Geometry on Detailed Heat Transfer Measurements over a HPT Turbine Blade Tip. *ASME Journal of Turbomachinery*, 126 (2004), 221-228.
 - 10 Ameri, A. A. and Steinthorsson, E. Prediction of Unshrouded Rotor Blade Tip Heat Transfer. *ICOMP-96-10* (1996).
 - 11 Ameri, A. A., Steinthorsson, E, and D, Rigby. Effect of Squealer Tip on Rotor Heat Transfer and Efficiency. *ASME Journal of Turbomachinery*, 120(4) (1998), 753-759.
 - 12 Krishnababu, S. K., Newton, P.J., Dawes, W. N., Lock, G. D., Hodson, H. P. Hannis, J., and Whitney, C. Aerothermal Investigation of Tip Leakage Flow in Axial Flow Turbines Part I - Effect of Tip Geometry and Tip Clearance Gap. *ASME Journal of Turbomachinery*, 131 (2009).
 - 13 Yang, H., Acharya, S., Ekkad, S. V., Prakash, C., and Bunker, R. Flow and Heat Transfer Predictions for a Flat-Tip Turbine Blade. *ASME Paper No. GT-2002-30190* (2002).
 - 14 Yang, H., Acharya, S., Ekkad, S. V., Prakash, C., and Bunker, R. Numerical Simulation of Flow and Heat Transfer Past a Turbine Blade With a Squealer-Tip. *ASME Paper No. GT-2002-30193* (2002).
 - 15 Yaras, M. L., Sjolander, S. A. Effects of Simulated Rotation on Tip Leakage in a Planar Cascade of Turbine Blades. *ASME Journal of Turbomachinery*, 114(3) (1992).
 - 16 Tallman, J. and Lakshminarayana, B. Numerical Simulation of Tip Leakage Flows in Axial Flow Turbines, With Emphasis on Flow Physics: Part II: Effect of Outer Casing Relative Motion. *ASME Journal of Turbomachinery*, 123(2) (2001), 324-333.
 - 17 Krishnababu, S.K., Dawes, W.N., Hodson, H.P., Lock, G.D., Hannis, J., and Whitney, C. Aero-Thermal Investigations of Tip Leakage Flow In Axial Flow Turbines: Part II—Effect of Relative Casing Motion. *ASME Journal of Turbomachinery*, 131(1) (2009).
 - 18 Yang, H., Chen, H.C., and Han, J.C. Turbine Rotor with Various Tip Configurations Flow and Heat Transfer Prediction. *Journal of thermophysics and heat transfer*, 20(1) (2006), 80-91.
 - 19 Mischo, B., Behr, T., and Abhari, R. S. Flow Physics and Profiling of Recessed Blade Tips: Impact on Performance and Heat Load. *AMSE Journal of Turbomachinery*, 130, 2 (2008).
 - 20 Zhou, C., Hodson, H., Tibbott, I., and Stokes, M. Effects of Endwall Motion on the Aero-thermal Performance of a Winglet Tip in a HP Turbine. *ASME Journal of Turbomachinery*, 134(6) (2012).
 - 21 Dunn, M. G. and Haldeman, C. W. Time-Averaged Heat Flux for a Recessed Tip, Lip, and Platform of a Transonic Turbine Blade. *ASME Journal of Turbomachinery*, 122(4) (2000), 692-698.
 - 22 Thorpe, S. J., Yoshino, S., Thomas, A. G., Ainsworth, R. W., and Harvey, N. Blade-Tip Heat Transfer in A Transonic Turbine. *Proceedings of the Institute of Mechanical Engineers Part A*, 219(6) (2005), 421-430.
 - 23 Molter, S. M., Dunn, M. G., Haldeman, C. W., Bergholz, R. F., and Vitt, P. Heat-flux Measurements and Predictions for the Blade Tip Region of a High-Pressure Turbine. *Proceedings of the ASME Turbo Expo*, 3 (2006), 49.
 - 24 Tallman, J. A., Haldeman, C. W., Dunn, M. G., Tolpadi, A. K., and Bergholz, R. F. Heat Transfer Measurements and Predictions for a Modern, High-Pressure, Transonic Turbine, Including Endwalls. *ASME Journal of Turbomachinery*, 131(2) (2009).
 - 25 Wheeler, A. P. S., Atkins, N. R., and He, L. Turbine Blade Tip Heat Transfer in Low Speed and High Speed Flows. *ASME Journal of Turbomachinery* , 133, 041025 (2011).
 - 26 Zhang, Q., O'Dowd, D. O., He, L., Wheeler, A. P. S., Ligrani, P. M., and Cheong, B. C. Y. Over-Tip Shock Wave Structure and Its Impact on Turbine Blade Tip Heat Transfer. *ASME Journal of Turbomachinery*, 133, 041001 (2011).
 - 27 Zhang, Q. and He, L. Overtip Choking and Its Implications on Turbine Blade-Tip Aerodynamic Performance. *Journal of Propulsion and Power*, 27(5) (2011), 1008-1014.
 - 28 Shyam, V., Ameri, A. A., and Chen, J. P. Analysis of Unsteady Tip and Endwall Heat Transfer in a Highly

Loaded Transonic Turbine Stage. *ASME Journal of Turbomachinery*, 134(4) (2011).

- 29 Zhang, Q., O'Dowd, D. O., He, L., Oldfield, M., and Ligrani, P. M. Transonic Turbine Blade Tip Aero-thermal Performance with Different Tip Gaps: Part I -- Tip Heat Transfer. *ASME Journal of Turbomachinery*, 133, 041027 (2011).
- 30 O'Dowd, D. O., Zhang, Q., He, L., Oldfield, M., Ligrani, M. P., Cheong, B. C. Y., and Tibbott, I. Aero-thermal Performance of a Winglet Tip at Engine Representative Mach and Reynolds Numbers. *ASME Journal of Turbomachinery*, 133 (2011).
- 31 Zhang, Q. and He, L. Tip-Shaping For HP Turbine Blade Aero-Thermal Performance Management. *ASME Paper No. GT-2012-68290* (2012).
- 32 He, L., Zhang, Q., Wheeler, A., Atkins, N. "An Aerofoil Structure (over-tip shaping for heat load reduction)", UK Patend, GB 1017797.0 (2010).
- 33 Shyam, V. and Ameri, A. A. Comparison of Various Supersonic Turbine Tip Designs to Minimize Aerodynamic Loss and Tip Heating. *ASME Paper No. GT-2011-46390* (2011).
- 34 O'Dowd, D. O., Zhang, Q., He, L., Ligrani, P. M., and Friedrichs, S. Comparison of Heat Transfer Measurement Techniques on a Transonic Turbine Blade Tip. *ASME Journal of Turbomachinery*, 133(2) (2011).
- 35 Oldfield, M. L. G. Impulse Response Processing of Transient Heat Transfer Gauge Signals. *ASME Journal of Turbomachinery*, 130(2) (2008).
- 36 O'Dowd, D. O., Zhang, Q., Usandizaga, I., He, L., & Ligrani, P. M. Transonic Turbine Blade Tip Aero-Thermal Performance With Different Tip Gaps: Part II—Tip Aerodynamic Loss. *ASME Paper No. GT2010-22780* (2010).
- 37 Zhang, Q., L. He, and A. Rawlinson. Effects of Inlet Turbulence and End-Wall Boundary Layer on Aerothermal Performance of a Transonic Turbine Blade Tip. *Journal of Engineering for Gas Turbines and Power* 136(5) (2014).